High Quantum Efficiencies in Polymer Solar Cells at Energy Losses below 0.6 eV

Weiwei Li,[*,†,‡] Koen H. Hendriks,[‡,§] Alice Furlan,[‡,§] Martijn M. Wienk,[‡,§] and René A. J. Janssen[*,‡,§]

[†]Beijing National Laboratory for Molecular Sciences, CAS Key Laboratory of Organic Solids, Institute of Chemistry, Chinese Academy of Sciences, Beijing 100190, P. R. China

[‡]Molecular Materials and Nanosystems, Institute of Complex Molecular Systems, Eindhoven University of Technology, P.O. Box 513, 5600 MB Eindhoven, The Netherlands

[§]Dutch Institute for Fundamental Energy Research, De Zaale 20, 5612 AJ Eindhoven, The Netherlands

Ⓢ *Supporting Information*

ABSTRACT: Diketopyrrolopyrrole-based conjugated polymers bridged with thiazole units and different donors have been designed for polymer solar cells. Quantum efficiencies above 50% have been achieved with energy loss between optical band gap and open-circuit voltage below 0.6 eV.

Conjugated polymers have been intensively investigated as electron donor in combination with fullerene acceptor derivatives in polymer solar cells (PSCs). Power conversion efficiencies (PCEs) above 10% have recently been obtained in single junction solar cells.[1−3] One of the main reasons that the performance of PSCs remains low compared to the best inorganic solution processed thin film solar cells, such as perovskite solar cells,[4,5] is the significant loss in energy of the open-circuit voltage (V_{oc}) relative to the optical band gap (E_g), determined from the onset of the linear absorption.[6] The minimum photon energy loss in PSCs defined as $E_{loss} = E_g - qV_{oc}$, has previously been suggested to be 0.6 eV.[7] In practice, the most efficient PCSs have $E_{loss} = 0.7−0.8$ eV. The trade-off is that when reducing E_{loss} to 0.6 eV, the quantum efficiency for charge generation often drops dramatically. In perovskite solar cells, E_{loss} is less than 0.5 eV.[8]

In PSCs the photon energy loss originates from a loss (∼0.5 eV) between V_{oc} and the energy of the charge-transfer (CT) state and from the energy difference between the singlet state (S1) of the polymer and the CT state (∼0.1 eV). While the minimum value for the latter can be close to 0.1 eV, or even less, the energy loss from S1 to CT state is ∼0.2−0.3 eV in the best cells. It has often been suggested that the photon energy loss may assist charge separation and enhance the efficiency of photon conversion into free charges. In Figure 1 we show how the external quantum efficiency (EQE) relates to E_{loss} for a range of successful polymers.

To further enhance the PCE of PSCs E_{loss} must be reduced, while keeping a high quantum efficiency for charge generation. Hence, polymers that approach and possibly fall below the 0.6 eV limit are required, but are rare.[9] Here we present the synthesis and application of conjugated polymers, designed to have a low photon energy loss, and demonstrate efficient charge generation in PSCs where $E_{loss} \leq 0.6$ eV.
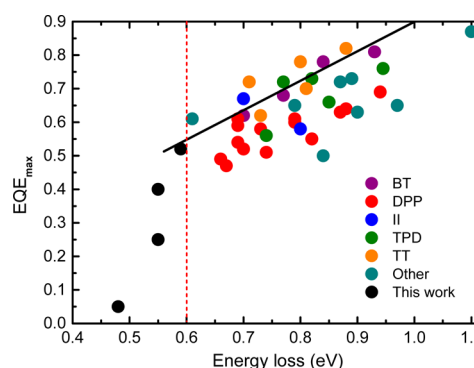

Figure 1. Maximum EQE within polymer absorption band vs the energy loss ($E_{loss} = E_g - qV_{oc}$) for published efficient conjugated polymer solar cells (see SI, Figure S1 for details). The lines are guides to the eye.

The most versatile design motif for tuning the optical band gap and redox energies of conjugated polymers is incorporating electron-rich and electron-deficient building blocks into an alternating polymer backbone. Strong electron-rich and electron-deficient units lower the optical band gap, by reducing the ionization potential (IP) and increasing the electron affinity (EA). The energy difference between the IP of the donor polymer and EA of the fullerene acceptor largely determines the V_{oc}.

In our design (Figure 2), we selected diketopyrrolopyrrole (DPP) units as electron deficient unit. DPPs have been successfully been applied in efficient near-infrared absorbing PSCs when substituted with thiophene on the 3 and 6 positions.[10] As we are interested in materials that provide a high V_{oc}, it is important to have a high IP. This can be achieved by replacing the electron-rich thiophene (T) rings with thiazoles (Tz) (Figure 2). The more electronegative nitrogen atom of thiazole increases the IP and EA of the polymer considerably. Recently, we reported on PDPP2TzT (Figure 2) where the EA was increased to such an extent that this polymer could be used as electron acceptor in all-polymer solar cells.[11] As electron donor PDPP2TzT gives a very low PCE with [70]PCBM as acceptor. To better adjust the IP and EA we thought to replace
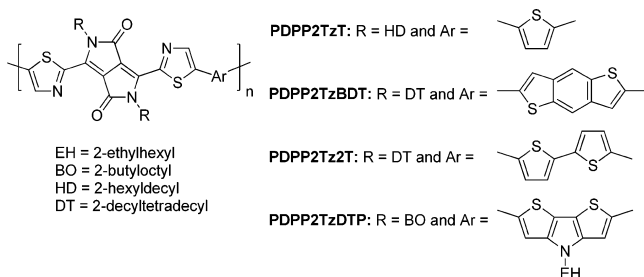
Figure 2. Thiazole-bridged diketopyrrolopyrrole-based conjugated polymers.

Figure 3. (a) Optical absorption spectra of the bisthiazole-DPP polymers in solid-state films. (b) Redox energies determined from cyclic voltammetry vs Fc/Fc⁺.

the thiophene ring in PDPP2TzT, by more electron-rich units such as benzodithiophene (BDT), bithiophene (2T), and dithienopyrrole (DTP) (Figure 2). With these new derivatives it is possible to make solar cells that still have $E_{loss} \leq 0.6$ eV, while having a significant quantum efficiency for charge generation. The results show that it is possible to create conjugated polymers for efficient charge generation in PSCs even with energy loss <0.6 eV.

The DPP polymers were synthesized from the bis(5-bromo-2-thiazoyl)-DPP monomer and the bisstannyl-donor monomers by Stille coupling polymerization using a $Pd_2(dba)_3/PPh_3$ (1:4) catalyst system in toluene/DMF (10:1) at 115 °C (Supporting Information (SI), Scheme S1). These reaction conditions have been developed to reduce side reactions and main-chain homocoupling defects.[12] It is also important to carefully select the alkyl side chains to approach the solubility limit which is important for optimized morphology in PSCs. In our design, 2-hexyldecyl (HD) side chains were applied in PDPP2TzT with thiophene as donor, longer 2-dodecyltetradecyl (DT) side chains for PDPP2TzBDT and PDPP2Tz2T, and 2-butyloctyl (BO) for PDPP2TzDTP. Combined with high molecular weights ranging from 76.0 to 108.9 kg/mol (Table 1,

Table 1. Molecular Weight and Optical and Electrochemical Properties of Thiazole-Bridged DPP Polymers

polymer	$M_n{}^a$ (kg/mol)	$E_g^{film}{}^b$ (eV)	$E_{red}{}^b$ (V)	$E_{ox}{}^b$ (V)	$\Delta E_{red}{}^c$ (eV)
PDPP2TzT	76.0	1.44	−1.16	0.74	0.07
PDPP2TzBDT	85.2	1.53	−1.23	0.71	0.16
PDPP2Tz2T	108.9	1.47	−1.28	0.66	0.21
PDPP2TzDTP	88.5	1.28	−1.29	0.38	0.22

^{a}Determined with GPC at 140 °C using o-DCB as the eluent. ^{b}Versus Fc/Fc⁺. $^c\Delta E_{red} = q(E_{red}([70]PCBM) − E_{red})$ with $E_{red}([70]PCBM) = −1.07$ V vs Fc/Fc⁺.

and SI, Figure S2) and the general tendency of DPP polymers to aggregate, the polymers were expected to provide the required nanoscale interpenetrating network when blended with [70]PCBM.[13]

The DPP polymers exhibit a strong near-infrared absorption (Figure 3a). The optical band gap determined from the onset of absorption decreases from $E_g = 1.53$ eV for BDT, to 1.47, 1.44, and 1.28 eV for the polymers with T, 2T, and DTP (Table 1). The redox energies of the polymers were determined by cyclic voltammetry on thin films (Figure 3b, Table 1, and SI, Figure S3) and reveal that PDPP2TzT has the highest oxidation potential (0.74 V) and a reduction potential at −1.16 V. Both the oxidation and reduction potentials decrease for the polymers with BDT, 2T, and DTP units. As shown in Table
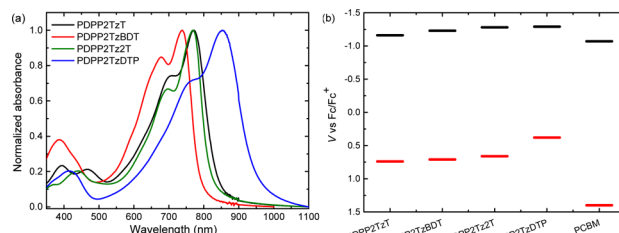
1, the difference in the reduction potentials (ΔE_{red}) for PDPP2TzT and [70]PCBM is only 0.07 eV, which is too small to result in photoinduced charge transfer. ΔE_{red} is slightly larger for the other three polymers ($\Delta E_{red} = 0.16-0.22$ eV). We note that this is still lower than 0.3 eV that is usually considered as threshold for efficient charge separation. For electron transfer, it is also important that the oxidation potentials differ. The oxidation potential of [70]PCBM is 1.4 V vs Fc/Fc⁺,[14] which makes that ΔE_{ox} is sufficiently large for the different polymers with respect to [70]PCBM (Figure 3b).

To test their performance as electron donor in solar cells, the DPP polymers were blended with [70]PCBM as electron acceptors. The layers were sandwiched between ITO/MoO₃ as hole collecting electrode and LiF/Al as electron collecting electrode. When using poly(3,4-ethylenedioxythiophene):poly-(styrenesulfonate) (PEDOT:PSS) instead of MoO₃, an s-shaped current density−voltage (J−V) characteristic was observed (SI, Figure S4 and Table S1) probably due to a detrimental interaction of acidic PSS⁻H⁺ with the basic imine nitrogen of the thiazole units.[15,16] We consider it less likely that the s-shape is caused by an insufficient work function contrast with the PEDOT:PSS, because the specific PEDOT:PSS formulation used provides V_{oc}'s in excess of 1 V, without s-shape for other polymer−fullerene cells.[17] Use of MoO₃ effectively removes the s-shape. The photoactive layers were carefully optimized by adjusting the solvent and cosolvent, the donor−acceptor ratio, and the layer thickness. For PDPP2TzT and PDPP2TzBDT the best performance was obtained for a polymer−fullerene weight ratio of 1:2 and spin coating the blend from chloroform with 10 vol % o-dichlorobenzene (o-DCB). For PDPP2Tz2T and PDPP2TzDTP the optimal polymer−fullerene weight ratio is 1:3 and spin coating from chloroform with 5 vol % o-DCB. The optimized thickness of these active layers is 105 nm. The J−V characteristics and EQE are shown in Figure 4, and the device parameters are summarized in Table 2. The J_{sc}'s were determined by integrating the EQE with the AM1.5G spectrum. The values correspond within 10% to those obtained from the J−V characteristics (SI, Table S2).

Despite a relatively high $V_{oc} = 0.96$ V, PDPP2TzT:[70]PCBM cells gave a very moderate PCE of 1.1% because of a low short-circuit current density ($J_{sc} = 2.0$ mA/cm²), which is associated with the very low $\Delta E_{red} = 0.07$ eV. For PDPP2TzBDT:[70]PCBM cells ΔE_{red} increases to 0.16 eV, which enhances the J_{sc} to 6.2 mA/cm² and PCE to 3.2%. The J_{sc} further increases to 8.8 mA/cm² for PDPP2Tz2T:[70]PCBM, where $\Delta E_{red} = 0.21$ eV resulting in PCE = 5.1%,. We note that despite low optical band gap of the PDPP2Tz2T ($E_g = 1.47$ eV), the $V_{oc} = 0.92$ V remains high. Finally, for PDPP2TzDTP:[70]PCBM cells with $\Delta E_{red} = 0.22$ eV, the PCE increases
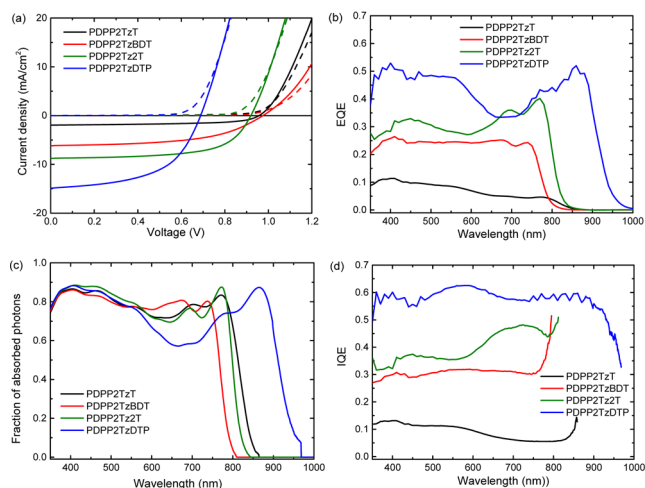
Figure 4. (a) $J-V$ characteristics in dark (dashed lines) and under simulated AM1.5G illumination (solid lines) of optimized solar cells of the DPP polymers with [70]PCBM. (b) EQE of the same devices (thickness of active layers is 105 nm). (c) Fraction of photons absorbed in the photoactive layers. (d) IQE of DPP polymer: [70]PCBM films.

Table 2. Characteristics of Optimized Solar Cells of the Thiazole-Bridged DPP Polymers with [70]PCBM[a]

polymer	J_{sc}[b] (mA/cm^2)	V_{oc} (V)	FF	PCE (%)	EQE	E_{loss} (eV)
PDPP2TzT[c]	2.0	0.96	0.58	1.1	0.05	0.48
PDPP2TzBDT[c]	6.2	0.98	0.53	3.2	0.25	0.55
PDPP2Tz2T[d]	8.8	0.92	0.63	5.1	0.40	0.55
PDPP2TzDTP[d]	14.9	0.69	0.54	5.6	0.52	0.59

[a]Measured under simulated AM1.5G illumination. [b]J_{sc} was calculated by integrating the EQE spectrum with the AM1.5G spectrum. The thickness of the active layers is 105 nm. The device configuration is ITO/MoO$_3$ (10 nm)/active layer/LiF/Al. [c]Weight ratio of the polymers to [70]PCBM is 1:2. The spin coating solvent is CHCl$_3$ with 10% o-DCB. [d]Weight ratio of the polymers to [70]PCBM is 1:3. The spin coating solvent is CHCl$_3$ with 5% o-DCB.

further to 5.6% with J_{sc} = 14.9 mA/cm^2. The FF of these cells is relatively low (0.53−0.63) when compared to other efficient DPP polymers despite the fact that the blends exhibit a fibrillar, semicrystalline polymer network microstructure in TEM (SI, Figure S5) that is typical for most DPP polymer:[70]PCBM blends.[13]

The different J_{sc}'s are also reflected in the EQE (Figure 4b). In the wavelength range where only the polymer absorbs, the PDPP2TzT:[70]PCBM cells give a maximum EQE of only 0.05. The EQE is further increased to 0.25, 0.40, and 0.52 for the other three polymers.

The EQE is determined by several factors. Recently we have shown that for DPP polymers a high EQE correlates with narrow polymer fibrils.[13] In accordance with this result the highest EQE is found for the PDPP2TzDTP:[70]PCBM blend, which has the finest morphology, while the other three appear more coarse (SI, Figure S5).

The other effect that we wish to study here is the effect of E_{loss}. Comparing Tables 1 and 2 reveals that the energy loss, E_{loss}, follows a similar trend as ΔE_{red} and also correlates with the EQE. For the PDPP2TzT:[70]PCBM cells where E_{loss} = 0.48 eV is the smallest, the EQE is very small, but for PDPP2TzDTP:[70]PCBM cells with E_{loss} = 0.59 eV the

maximum EQE increases to 0.52. PDPP2TzBDT:[70]PCBM and PDPP2Tz2T:[70]PCBM have the same energy loss E_{loss} = 0.55 eV, but the latter shows a higher EQE and high PCE. The results, however, still follow the trend of an enhanced EQE with larger E_{loss} as shown in Figure 1.[18] The EQE of 0.52 obtained in this work for PDPP2TzDTP:[70]PCBM at E_{loss} = 0.59 eV, is higher than the best other DPP polymer PDPP3T with maximum EQE of 0.49 at an E_{loss} = 0.65 eV.[10] A similar low E_{loss} polymer was recently reported by Bazan and co-workers: a regioregular PIPCP polymer with E_{loss} = 0.61 eV gave EQE = 0.61.[19]

While the EQE is readily available from literature data, the internal quantum efficiency (IQE) is of course a more relevant parameter for comparing different materials. The IQE of the cells was determined by dividing the EQE by the fraction of photons absorbed as determined from optical modeling of the device stack using the wavelength dependent refractive index (n) and extinction coefficients (k) of all layers involved (SI, Figure S6). With a thickness of 105 nm, these blends absorb up to 90% of the light at the peak absorption (Figure 4c). The IQE follows the similar trend as the maximum EQE in these PSCs (Figure 4d). The integrated IQE over the absorption region is 0.09, 0.31, 0.41, and 0.59 for the solar cells based on polymers PDPP2TzT, PDPP2TzBDT, PDPP2Tz2T, and PDPP2TzDTP.

The high EQE and IQE at E_{loss} < 0.6 eV of these thiazole-bridged DPP polymers seem to break the E_{loss} limit of 0.6 eV.[7] The redox potentials of these polymers were designed to have a low ΔE_{red} in combination with a high oxidation potential such that V_{oc} could be optimized with respect to E_g. Although cells with a relatively low E_{loss} were obtained, further improvements are needed to improve the moderately high EQE. There are several mechanisms that can contribute to a low E_{loss} while maintaining a high EQE. Among these are reducing energetic disorder,[20,21] eliminating main chain defects or reactive end groups that can trap charges,[12] reducing the recombination of free carriers by reducing the donor−acceptor interface area,[22] and increasing the dielectric constant.[23,24] Apart from, the careful design of redox energies, addressing these issues in novel materials design is imperative to increase the efficiency of organic solar cells beyond the 11% level.

In conclusion, we successfully designed and synthesized several DPP polymers bridged with thiazole for PSCs. The photovoltaic devices based on these polymers gave high EQE up to 0.52 and PCE up to 5.6% with low energy loss <0.6 eV. The results indicate the possibility to further enhance the efficiency limit by reducing the energy loss for PSCs.

■ ASSOCIATED CONTENT

Ⓢ Supporting Information

Experimental details and characterization data. This material is available free of charge via the Internet at http://pubs.acs.org.

■ AUTHOR INFORMATION

Corresponding Authors

*liweiwei@iccas.ac.cn
*r.a.j.janssen@tue.nl

Notes

The authors declare no competing financial interest.

■ ACKNOWLEDGMENTS

■ REFERENCES

(1) Liu, Y.; Zhao, J.; Li, Z.; Mu, C.; Ma, W.; Hu, H.; Jiang, K.; Lin, H.; Ade, H.; Yan, H. *Nat. Commun.* **2014**, *5*, 5293/1−8.

(2) Chen, J.-D.; Cui, C.; Li, Y.-Q.; Zhou, L.; Ou, Q.-D.; Li, C.; Li, Y.; Tang, J.-X. *Adv. Mater.* **2015**, *27*, 1035−1041.

(3) Lia, S.-H.; Jhuo, H.-J.; Yeh, P.-N.; Cheng, Y.-S.; Li, Y.-L.; Lee, Y.-H.; Sharma, S.; Chen, S.-A. *Sci. Rep.* **2014**, *4*, 6813/1−7.

(4) Green, M. A.; Ho-Baillie, A.; Snaith, H. J. *Nat. Photon.* **2014**, *8*, 506−514.

(5) Marchioro, A.; Teuscher, J.; Friedrich, D.; Kunst, M.; van de Krol, R.; Moehl, T.; Gratzel, M.; Moser, J.-E. *Nat. Photon.* **2014**, *8*, 250−255.

(6) Janssen, R. A. J.; Nelson, J. *Adv. Mater.* **2012**, *25*, 1847−1858.

(7) Veldman, D.; Meskers, S. C. J.; Janssen, R. A. J. *Adv. Funct. Mater.* **2009**, *19*, 1939−1948.

(8) Nayak, P. K.; Cahen, D. *Adv. Mater.* **2014**, *26*, 1622−1628.

(9) Sonar, P.; Singh, S. P.; Li, Y.; Soh, M. S.; Dodabalapur, A. *Adv. Mater.* **2010**, *22*, 5409−5413.

(10) Hendriks, K. H.; Heintges, G. H. L.; Gevaerts, V. S.; Wienk, M. M.; Janssen, R. A. J. *Angew. Chem., Int. Ed.* **2013**, *52*, 8341−8344.

(11) Li, W.; Roelofs, W. S. C.; Turbiez, M.; Wienk, M. M.; Janssen, R. A. J. *Adv. Mater.* **2014**, *26*, 3304−3309.

(12) Hendriks, K. H.; Li, W.; Heintges, G. H. L.; van Pruissen, G. W. P.; Wienk, M. M.; Janssen, R. A. J. *J. Am. Chem. Soc.* **2014**, *136*, 11128−11133.

(13) Li, W.; Hendriks, K. H.; Furlan, A.; Roelofs, W. S. C.; Wienk, M. M.; Janssen, R. A. J. *J. Am. Chem. Soc.* **2013**, *135*, 18942−18948.

(14) Hellström, S.; Zhang, F.; Inganäs, O.; Andersson, M. R. *Dalton Trans.* **2009**, 10032−10039.

(15) Garcia, A.; Welch, G. C.; Ratcliff, E. L.; Ginley, D. S.; Bazan, G. C.; Olson, D. C. *Adv. Mater.* **2012**, *24*, 5368−5373.

(16) Sakthivel, P.; Kranthiraja, K.; Saravanan, C.; Gunasekar, K.; Kim, H. I.; Shin, W. S.; Jeong, J.-E.; Woo, H. Y.; Jin, S.-H. *J. Mater. Chem. A* **2014**, *2*, 6916−6921.

(17) Esiner, S.; van Eersel, H.; Wienk, M. M.; Janssen, R. A. J. *Adv. Mater.* **2013**, *25*, 2932−2936.

(18) Li, W.; Roelofs, W. S. C.; Wienk, M. M.; Janssen, R. A. J. *J. Am. Chem. Soc.* **2012**, *134*, 13787−13795.

(19) Wang, M.; Wang, H.; Yokoyama, T.; Liu, X.; Huang, Y.; Zhang, Y.; Nguyen, T.-Q.; Aramaki, S.; Bazan, G. C. *J. Am. Chem. Soc.* **2014**, *136*, 12576−12579.

(20) Blakesley, J. C.; Neher, D. *Phys. Rev. B* **2011**, *84*, 075210/1−12.

(21) Garcia-Belmonte, G.; Bisquert, J. *Appl. Phys. Lett.* **2010**, *96*, 113301/1−3.

(22) Vandewal, K.; Widmer, J.; Heumueller, T.; Brabec, C. J.; McGehee, M. D.; Leo, K.; Riede, M.; Salleo, A. *Adv. Mater.* **2014**, *26*, 3839−3843.

(23) Chen, S.; Tsang, S.-W.; Lai, T.-H.; Reynolds, J. R.; So, F. *Adv. Mater.* **2014**, *26*, 6125−6131.

(24) Koster, L. J. A.; Shaheen, S. E.; Hummelen, J. C. *Adv. Energy Mater.* **2012**, *2*, 1246−1253.